

Decoherence due to Elastic Rayleigh Scattering

H. Uys,^{1,2,*} M. J. Biercuk,^{1,3} A. P. VanDevender,¹ C. Ospelkaus,¹ D. Meiser,⁴ R. Ozeri,⁵ and J. J. Bollinger^{1,†}

¹National Institute of Standards and Technology, Boulder, Colorado 80305, USA

²Council for Scientific and Industrial Research, Pretoria, South Africa

³School of Physics, University of Sydney 2006, Australia

⁴JILA and Department of Physics, University of Colorado, Boulder, Colorado 80309-0440, USA

⁵Department of Physics of Complex Systems, Weizmann Institute of Science, Rehovot, Israel

(Received 9 July 2010; published 8 November 2010)

We present theoretical and experimental studies of the decoherence of hyperfine ground-state superpositions due to elastic Rayleigh scattering of light off resonant with higher lying excited states. We demonstrate that under appropriate conditions, elastic Rayleigh scattering can be the dominant source of decoherence, contrary to previous discussions in the literature. We show that the elastic-scattering decoherence rate of a two-level system is given by the square of the difference between the elastic-scattering *amplitudes* for the two levels, and that for certain detunings of the light, the amplitudes can interfere constructively even when the elastic-scattering *rates* from the two levels are equal. We confirm this prediction through calculations and measurements of the total decoherence rate for a superposition of the valence electron spin levels in the ground state of $^9\text{Be}^+$ in a 4.5 T magnetic field.

DOI: 10.1103/PhysRevLett.105.200401

PACS numbers: 03.65.Yz, 37.10.Ty, 42.50.-p

Off-resonant light scattering (spontaneous emission) is an important source of decoherence in many coherent-control experiments with atoms and molecules. Examples include the use of optical-dipole forces for gates in quantum computing [1], the generation of spin squeezed states through laser-mediated interactions [2–6], and the trapping and manipulation of neutral atoms in optical lattices [7,8]. These experiments frequently involve superpositions of two-level atomic systems (qubits) and use laser beams off resonant with higher lying excited states to control and measure the atomic states.

In general, decoherence of an atomic superposition state due to off-resonant light scattering occurs if the scattered photon carries information about the qubit state. During Raman scattering the initial and final qubit states differ. The state of the scattered photon is entangled with the atomic state, providing “welcher-Weg” (which-way) information and leading to decoherence [9,10]. By contrast the role of elastic Rayleigh scattering for decoherence is not as clear. Two very different regimes have been discussed and are supported by experiment. On the one hand it has been found that in some experiments Rayleigh scattering gives rise to negligible decoherence provided that the elastic-scattering rates from both qubit levels are approximately equal [10]. On the other hand, decoherence due to Rayleigh scattering of photons on a cycling transition is used for strong projective state measurement [11].

In this Letter we develop a microscopic theory for the decoherence of a qubit due to elastic Rayleigh scattering that gives a unified treatment of these different regimes. Our key finding is that decoherence induced by Rayleigh scattering is proportional to the square of the difference of the probability *amplitudes* for elastic scattering from the

two levels [Eq. (7)]. When the two amplitudes are approximately equal the resulting decoherence rate can be small (first case above) and when one amplitude dominates the other, Rayleigh decoherence can be large (second case above). However, even when the elastic scatter rates are approximately equal, the scattering amplitudes can have opposite sign—a situation applicable to many coherent-control experiments [2–6]—and Rayleigh decoherence can still dominate Raman decoherence.

In the rest of this Letter we derive the microscopic model that quantitatively describes the decoherence due to Rayleigh scattering and verify our predictions against an experiment with $^9\text{Be}^+$ in a 4.5 T magnetic field. For concreteness we discuss the problem in terms of the relevant energy level structure of $^9\text{Be}^+$ shown in Fig. 1. The two ground-state sublevels $|u\rangle = |+\frac{1}{2}\rangle$ and $|d\rangle = |-\frac{1}{2}\rangle$ corresponding to the valence electron spin states parallel and antiparallel to an applied magnetic field are split by $\Omega_z/(2\pi) = 124.1$ GHz. Also shown are the first excited P state levels $|J, M_J\rangle$, $J = \frac{3}{2}, \frac{1}{2}$. We consider a nonresonant light field $(\sum_{\lambda=-1}^1 b_{\lambda} \hat{\epsilon}_{\lambda}) \mathcal{E}_0 \cos(\mathbf{k}_0 \cdot \mathbf{x} - \omega_0 t)$, where b_{λ} is the amplitude of the corresponding polarization component $\hat{\epsilon}_{\lambda}$ of the light, and derive a master equation for the time evolution of the $|\pm\frac{1}{2}\rangle$ ground-state sublevels in the presence of the off-resonant light.

An effective Hamiltonian coupling of the two qubit levels via spontaneous scattering of the driving field into the vacuum modes can be derived by adiabatic elimination of the excited states shown in Fig. 1 and is given by

$$H_{sp} = H_{dd} + H_{uu} + H_{du} + H_{ud}. \quad (1)$$

Here the different terms describe processes which either do, or do not, flip the atomic spin upon scattering of a

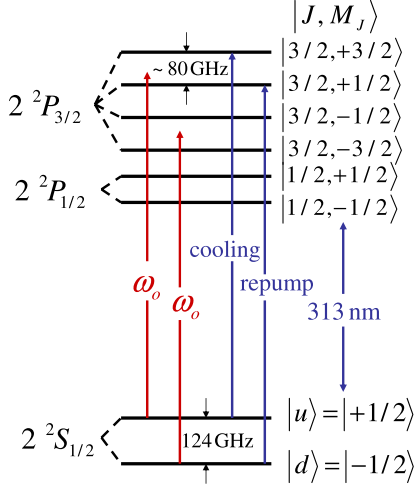


FIG. 1 (color online). Relevant energy level structure of ${}^9\text{Be}^+$ at 4.5 T. We only show the $m_l = +\frac{3}{2}$ levels which are prepared experimentally though optical pumping. The off-resonant laser is shown with a frequency ω_o appropriate for the experimental results presented in Fig. 3.

photon, as indicated by the subscripts. The Raman terms that lead to spin-flips are (in the Schrödinger picture),

$$H_{du} = \hbar \sum_{Jk\lambda} (h_{Jk\lambda}^{du} \hat{\sigma}^- \hat{a}_{k\lambda} E^-(\Delta\mathbf{k}) + h_{Jk\lambda}^{du*} \hat{\sigma}^+ \hat{a}_{k\lambda}^\dagger E^+(\Delta\mathbf{k}))$$

$$H_{ud} = \hbar \sum_{Jk\lambda} (h_{Jk\lambda}^{ud} \hat{\sigma}^- \hat{a}_{k\lambda}^\dagger E^+(\Delta\mathbf{k}) + h_{Jk\lambda}^{ud*} \hat{\sigma}^+ \hat{a}_{k\lambda} E^-(\Delta\mathbf{k})),$$

where $\hat{a}_{k\lambda}^\dagger$ ($\hat{a}_{k\lambda}$) is the raising (lowering) operator for the \mathbf{k} , λ mode of the electromagnetic field, $\hat{\sigma}^+ = (\hat{\sigma}_x + i\hat{\sigma}_y)/2$ and $\hat{\sigma}^- = (\hat{\sigma}_x - i\hat{\sigma}_y)/2$ where σ_x , σ_y , and σ_z are the Pauli matrices for the two-level ground state, and $E^+(\Delta\mathbf{k}) = E^{*-}(\Delta\mathbf{k}) = (\mathcal{E}_0/2)e^{i(\mathbf{k}_0 - \mathbf{k}) \cdot \mathbf{x} - i\omega_0 t}$. The coupling constants are

$$h_{Jk\lambda}^{ij} = -\frac{b_\lambda g_{\mathbf{k}}}{\hbar^2 \delta_{ij\lambda}} \langle i | \mathbf{d} \cdot \hat{\mathbf{e}}_{\lambda}^* | J, \lambda + i \rangle \langle J, \lambda + i | \mathbf{d} \cdot \hat{\mathbf{e}}_{\lambda + (i-j)} | j \rangle,$$

where $i, j \in \{-\frac{1}{2}, \frac{1}{2}\}$, $\delta_{ij\lambda} = \Omega_{J, \lambda+i} - \Omega_i - \omega_0$ is the detuning of ω_0 from the $|i\rangle \rightarrow |J, M_J = \lambda + i\rangle$ transition, at energies $\hbar\Omega_i$ and $\hbar\Omega_{J, \lambda+i}$ respectively, and $g_{\mathbf{k}} = \sqrt{\hbar\omega_{\mathbf{k}}/(2\epsilon_0 V)}$ with V the quantization volume. Similarly, the Rayleigh terms are

$$H_{dd} = \hbar \sum_{Jk\lambda} (h_{Jk\lambda}^{dd} \hat{a}_{k\lambda} E^-(\Delta\mathbf{k}) + h_{Jk\lambda}^{dd*} \hat{a}_{k\lambda}^\dagger E^+(\Delta\mathbf{k})) \hat{\sigma}_1,$$

$$H_{uu} = \hbar \sum_{Jk\lambda} (h_{Jk\lambda}^{uu} \hat{a}_{k\lambda} E^-(\Delta\mathbf{k}) + h_{Jk\lambda}^{uu*} \hat{a}_{k\lambda}^\dagger E^+(\Delta\mathbf{k})) \hat{\sigma}_2,$$

where we have defined the operators $\hat{\sigma}_1 = \frac{1}{2}(I - \sigma_z) = |d\rangle\langle d|$, $\hat{\sigma}_2 = \frac{1}{2}(I + \sigma_z) = |u\rangle\langle u|$. The Rayleigh terms can be combined into $H_{\text{el}} = H_{dd} + H_{uu}$, where

$$H_{\text{el}} = \frac{\hbar}{2} \sum_{Jk\lambda} (h_{Jk\lambda}^{dd} + h_{Jk\lambda}^{uu}) \hat{a}_{k\lambda} E^-(\Delta\mathbf{k}) - \frac{\hbar}{2} \hat{\sigma}_z \sum_{Jk\lambda} (h_{Jk\lambda}^{dd} - h_{Jk\lambda}^{uu}) \hat{a}_{k\lambda} E^-(\Delta\mathbf{k}) + \text{H.c.} \quad (2)$$

The first term in Eq. (2) is proportional to the identity for the qubit and produces no decoherence. The second term proportional to $\hat{\sigma}_z$ leads to dephasing which, as we will see, can be the dominant decohering process.

The time evolution of the reduced density matrix, $\tilde{\rho}_S(t')$, of the qubit is well described by the master equation [12]

$$\frac{\partial \tilde{\rho}_S(t)}{\partial t} = -\frac{1}{\hbar^2} \int_0^t dt' \text{Tr}_{\mathbf{k}} \{ [H_{\text{sp}}(t), [H_{\text{sp}}(t'), \rho_S(t') \rho_{\mathbf{k}}]] \}, \quad (3)$$

in which $\rho_S(t')$ is the density matrix of the qubit before tracing over all vacuum modes represented by density matrix $\rho_{\mathbf{k}}$ as indicated by $\text{Tr}_{\mathbf{k}}$.

In evaluating Eq. (3) we find Raman scattering terms given in the Lindblad form by [13]

$$\begin{aligned} \mathcal{L}_{du} \tilde{\rho}_S(t) &= -\frac{\Gamma_{du}}{2} (\hat{\sigma}^- \hat{\sigma}^+ \tilde{\rho}_S(t) - 2\hat{\sigma}^+ \tilde{\rho}_S(t) \hat{\sigma}^- \\ &\quad + \tilde{\rho}_S(t) \hat{\sigma}^- \hat{\sigma}^+), \\ \mathcal{L}_{ud} \tilde{\rho}_S(t) &= -\frac{\Gamma_{ud}}{2} (\hat{\sigma}^+ \hat{\sigma}^- \tilde{\rho}_S(t) - 2\hat{\sigma}^- \tilde{\rho}_S(t) \hat{\sigma}^+ \\ &\quad + \tilde{\rho}_S(t) \hat{\sigma}^+ \hat{\sigma}^-). \end{aligned}$$

Γ_{ij} is the rate for an ion initially in state $|i\rangle$ to scatter a photon and end up in state $|j\rangle$ and is given by the Kramers-Heisenberg formula

$$\Gamma_{ij} = \Omega_R^2 \gamma \sum_{\lambda} \left(\sum_J A_{J, \lambda}^{i \rightarrow j} \right)^2. \quad (4)$$

Here $\Omega_R = \mu \mathcal{E}_0 / (2\hbar)$, γ is the spontaneous decay rate of the excited states, and the amplitudes $A_{J, \lambda}^{i \rightarrow j}$ for scattering through intermediate level $|J, \lambda + i\rangle$ are defined as

$$A_{J, \lambda}^{i \rightarrow j} = \frac{b_\lambda \langle j | \mathbf{d} \cdot \hat{\mathbf{e}}_{\lambda + (i-j)}^* | J, \lambda + i \rangle \langle J, \lambda + i | \mathbf{d} \cdot \hat{\mathbf{e}}_{\lambda} | i \rangle}{\delta_{ij\lambda} \mu^2}, \quad (5)$$

where $\mu = \langle \frac{3}{2}, \frac{3}{2} | \mathbf{d} \cdot \hat{\mathbf{e}}_1 | \frac{1}{2} \rangle$ is the largest dipole matrix element. We define the total Raman scattering rate $\Gamma_{\text{Ram}} = \Gamma_{du} + \Gamma_{ud}$.

The contributions to Eq. (3) from Rayleigh scattering are

$$\mathcal{L}_{dd,uu} \tilde{\rho}_S(t) = -\frac{\Gamma_{\text{el}}}{4} [\tilde{\rho}_S(t) - \hat{\sigma}_z \tilde{\rho}_S(t) \hat{\sigma}_z], \quad (6)$$

where

$$\Gamma_{\text{el}} = \Omega_R^2 \gamma \sum_{\lambda} \left(\sum_J A_{J, \lambda}^{d \rightarrow d} - \sum_{J'} A_{J', \lambda}^{u \rightarrow u} \right)^2. \quad (7)$$

Finally, the full time evolution of the reduced density matrix is $\frac{\partial \tilde{\rho}_S(t)}{\partial t} = (\mathcal{L}_{du} + \mathcal{L}_{ud} + \mathcal{L}_{dd,uu}) \tilde{\rho}_S(t)$. With

$$\tilde{\rho}_S(t) \equiv \begin{pmatrix} \rho_{uu} & \rho_{ud} \\ \rho_{du} & \rho_{dd} \end{pmatrix}$$

this can be written as

$$\frac{\partial \tilde{\rho}_S(t)}{\partial t} = \begin{pmatrix} -\Gamma_{ud}\rho_{uu} + \Gamma_{du}\rho_{dd} & -\frac{1}{2}(\Gamma_{\text{Ram}} + \Gamma_{\text{el}})\rho_{ud} \\ -\frac{1}{2}(\Gamma_{\text{Ram}} + \Gamma_{\text{el}})\rho_{du} & -\Gamma_{du}\rho_{dd} + \Gamma_{ud}\rho_{uu} \end{pmatrix}. \quad (8)$$

Equation (7) is the main theoretical result of this Letter. General master equation treatments of decoherence due to elastic scattering have appeared in the literature [14]. However, to our knowledge this is the first calculation producing a simple formula which demonstrates the central role of elastic-scattering amplitudes in spontaneous-emission-induced decoherence of hyperfine-state superpositions.

Since the detunings in the two amplitudes in Eq. (7) can have opposite sign, the different contributions can add constructively, leading to a large Rayleigh scattering decoherence. Physically the term proportional to $\hat{\sigma}_z$ in Eq. (2) suggests that this decoherence is due to dephasing. A photon elastically scattered into mode \mathbf{k} , λ produces a shift in the phase of a superposition of the $|u\rangle$, $|d\rangle$ levels proportional to the difference in the amplitudes for scattering into that mode. Photons scattering at random times and into random directions produce random phase shifts and a loss of phase information.

We realize elastic-scattering amplitudes with opposite sign in a Penning ion trap operating in the strong-field Zeeman regime. These traps have found increasing importance in quantum information studies [15–17], underscoring the need for quantitative analysis of decoherence processes in these systems. Details of our basic Penning trap setup can be found in [18]. We use two 313 nm laser beams (see Fig. 1) to Doppler laser cool ($T \sim 0.5$ mK) and optically pump a planar crystal (diameter ~ 300 μm) of ~ 100 $^9\text{Be}^+$ ions into the $|u\rangle = |1/2\rangle$ state. A phase-locked Gunn diode oscillator near 124 GHz provides microwave radiation used to perform high-fidelity ($> 99\%$) qubit rotations. At the end of an experiment, the population in the $|u\rangle$ state is measured by detecting the resonantly scattered ion fluorescence induced by the Doppler cooling laser (tuned to the $|u\rangle \rightarrow |3/2, 3/2\rangle$ cycling transition), and normalizing this fluorescence level to that obtained with all the ions in $|u\rangle$.

We introduce an off-resonant, linearly polarized laser beam and measure the total decoherence rate $\frac{1}{2} \times (\Gamma_{\text{Ram}} + \Gamma_{\text{el}})$ from a decrease in length of the composite Bloch vector of the ions using a two- π -pulse spin-echo sequence like that shown in Fig. 2(a). In this sequence the relative phases of the $\pi/2$ and π pulses are shifted by 90° , in which case in the absence of decoherence all ions are rotated to $|d\rangle$ at the end of the sequence. The measured population in $|u\rangle$ therefore provides a measure of the total decoherence. From Eq. (8) we calculate that at the end of the spin-echo sequence $\rho_{uu} = \frac{1}{2}(1 - e^{-(\Gamma_{\text{Ram}} + \Gamma_{\text{el}})\tau/2})$, where τ is the total laser interaction time of the spin-echo sequence. Figure 2(d) shows measurements of the $|u\rangle$ state population as a function of the spin-echo laser interaction time. We determine $\frac{1}{2}(\Gamma_{\text{Ram}} + \Gamma_{\text{el}})$ from the fitted slope at short spin-echo sequence times.

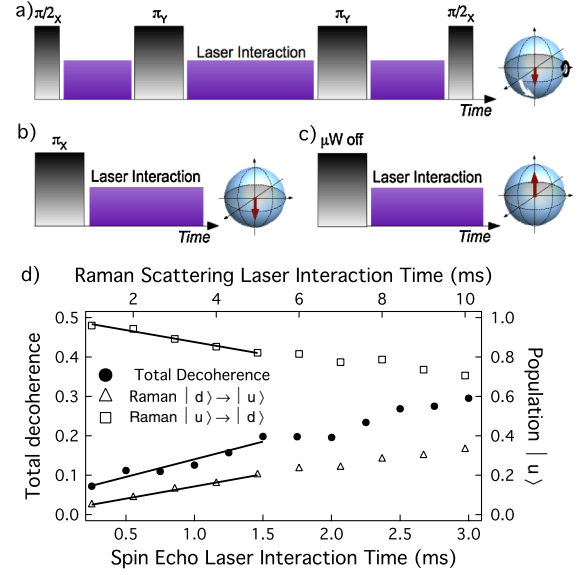


FIG. 2 (color online). (a)–(c) Schematic pulse sequences used to measure (a) total decoherence and (b), (c) Raman scattering rates. Raman scatter rates Γ_{du} and Γ_{ud} (used to calibrate laser intensity, see Fig. 3) obtained by initializing the ions in $|d\rangle$ or $|u\rangle$ respectively and measuring the $|u\rangle$ state population vs off-resonant laser interaction time. (d) Example measurements of the total decoherence and Raman scatter rates. Left axis: Total decoherence (solid markers); Right axis: Population measured in $|u\rangle$ to determine Raman scattering rates (open markers). Solid lines are fits to the data from which the Raman scattering and decoherence rates were extracted.

Other sources of decoherence can be neglected. Without off-resonant light we measure a $\sim 1\%$ loss in coherence due to magnetic field fluctuations for up to 6 ms spin-echo times, much longer than the sequence times used to determine decoherence due to off-resonant light scattering. Further, the differential ac-stark shift from the off-resonant laser is nulled to better than 1 kHz by rotating the polarization. Doing so minimizes decoherence due to laser-power fluctuations. Electric field homogeneity due to the laser beam waist is greater than 95% over the ion planar array.

Figure 3(a) presents two sets of measurements of the total decoherence rate as a function of the frequency of the off-resonant light, and compares these measurements with different theoretical predictions. For these measurements the intermediate state detunings and resulting $d \rightarrow d$ and $u \rightarrow u$ scattering amplitudes in Eq. (7) have opposite sign, producing a large elastic decoherence rate. This condition is in part achieved because the light detunings to the intermediate $P_{3/2}$ levels are comparable to the large (124 GHz) qubit splitting.

The two measurement sets use different ion crystals and different techniques for calibrating the off-resonant light intensity [see Figs. 3(b) and 3(c)]. Good agreement is obtained with the full theory presented here which manifests a Rayleigh decoherence rate determined by the square of the difference between the $|u\rangle$ and $|d\rangle$ elastic-scattering amplitudes [Eq. (7)]. This contrasts with the idea conveyed

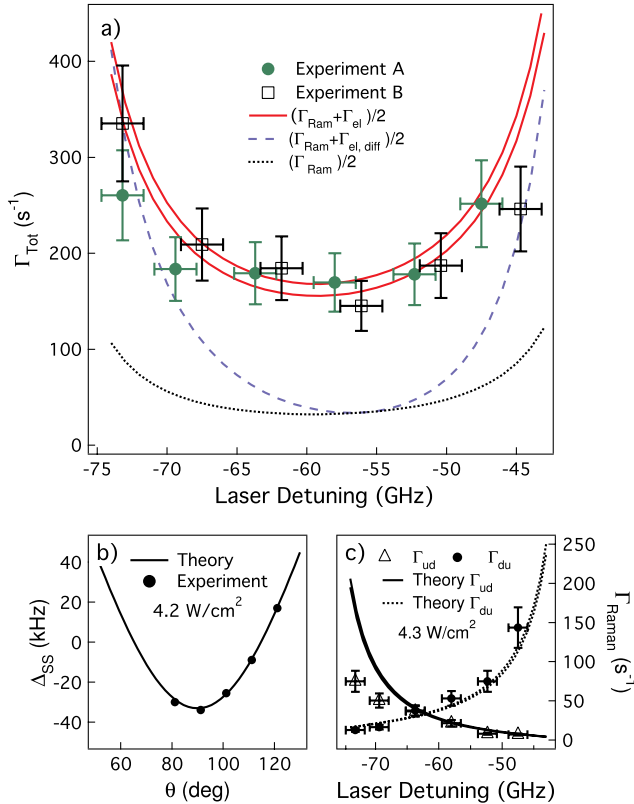


FIG. 3 (color online). (a) Comparison of the total decoherence rate with different theoretical models as a function of light detuning from the $|u\rangle \rightarrow |3/2, 3/2\rangle$ cycling transition for two independent sets of measurements. The light intensity was calibrated through fits to (b) light shift measurements of the qubit transition vs the polarization angle (experiment A) and (c) Raman scatter rates (experiment B). The full theory developed in this Letter agrees with the experimental data for all detunings while a theory accounting only for decoherence due to Raman transitions significantly underestimates the decoherence rate and an estimate based on scattering rate differences ($\Gamma_{\text{el,diff}}$) agrees with experiment only near the $|u\rangle \rightarrow |3/2, 1/2\rangle$ and $|d\rangle \rightarrow |3/2, -1/2\rangle$ resonances at -79.4 and -37.7 GHz, respectively. The difference in the two full theory curves is due to uncertainty in the laser polarization and absolute laser intensity calibration.

in previous literature that decoherence due to elastic scattering is produced by a difference in elastic-scattering rates. For example, Ref. [19] (Sec. III.B) discusses the which-way information acquired due to a difference in Rayleigh scattering rates and estimates a decoherence rate $\frac{1}{2}\Gamma_{\text{el,diff}} = \frac{(\Gamma_{uu} - \Gamma_{dd})^2}{(\Gamma_{uu} + \Gamma_{dd})}$ due to these rate differences. Figure 3(a) shows theory based on $\Gamma_{\text{el,diff}}$. As the laser detuning approaches resonant transitions at -79.4 GHz and -37.7 GHz, reasonable agreement is obtained with this theory. However, at a detuning of ~ -56 GHz, $\Gamma_{uu} \approx \Gamma_{dd}$ and we measure a decoherence rate that is 5 times larger than that predicted by $\frac{1}{2}(\Gamma_{\text{Ram}} + \Gamma_{\text{el,diff}})$.

These measurements can be contrasted with previous work [10] using trapped $^9\text{Be}^+$ ions at low magnetic field in which Rayleigh-scattering-induced decoherence was shown to be negligible. The results of that experiment

benefited from some fortuitous conditions: the detuning Δ of the light from any atomic excited state was large compared to the qubit transition frequency, and the qubit states were clock states (states whose energy difference does not depend to first order on changes in the magnetic field). These conditions imply a nearly complete cancellation of the elastic-scattering amplitudes in Eq. (7) resulting in a weak Rayleigh decoherence with a dependence on detuning $\propto 1/\Delta^4$. For general two-level systems the cancellation will not be as complete, resulting in a Rayleigh decoherence rate $\propto 1/\Delta^2$. The prescription discussed in this manuscript now enables an accurate calculation of Rayleigh decoherence for these low-field trapped ion as well as other coherent-control experiments.

We thank W.M. Itano, J.P. Britton, D. Hanneke, and M. J. Holland for useful suggestions. M. J. B. acknowledges support from Georgia Tech and IARPA. D. M. is supported by NSF. This work was supported by the DARPA OLE program and by IARPA. This manuscript is the contribution of NIST and is not subject to U.S. copyright.

*huys@csir.co.za

†john.bollinger@nist.gov

- [1] R. Blatt and D.J. Wineland, *Nature (London)* **453**, 1008 (2008).
- [2] J. Appel *et al.*, *Proc. Natl. Acad. Sci. U.S.A.* **106**, 10960 (2009).
- [3] I. D. Leroux, M. H. Schleier-Smith, and V. Vuletić, *Phys. Rev. Lett.* **104**, 073602 (2010).
- [4] S. Chaudhury, G. A. Smith, K. Schulz, and P. S. Jessen, *Phys. Rev. Lett.* **96**, 043001 (2006).
- [5] I. Teper, G. Vrijsen, J. Lee, and M. A. Kasevich, *Phys. Rev. A* **78**, 051803 (2008).
- [6] J. M. Geremia, J. K. Stockton, and H. Mabuchi, *Phys. Rev. A* **73**, 042112 (2006).
- [7] H. Katori, M. Takamoto, V. G. Palchikov, and V. D. Ovsianikov, *Phys. Rev. Lett.* **91**, 173005 (2003).
- [8] B. Mischuck, I. H. Deutsch, and P. S. Jessen, *Phys. Rev. A* **81**, 023403 (2010).
- [9] D. L. Moehring, M. J. Madsen, B. B. Blinov, and C. Monroe, *Phys. Rev. Lett.* **93**, 090410 (2004).
- [10] R. Ozeri *et al.*, *Phys. Rev. Lett.* **95**, 030403 (2005).
- [11] A. H. Myerson *et al.*, *Phys. Rev. Lett.* **100**, 200502 (2008).
- [12] C. W. Gardiner and P. Zoller, *Quantum Noise* (Springer-Verlag, Berlin Heidelberg, 2002), p. 140, 2nd ed.
- [13] When multiplying out the double commutator in Eq. (3) all products involving different terms of H_{el} , H_{ud} , or H_{du} are neglected because they are rapidly oscillating of order Ω_z (secular approximation).
- [14] C. Cohen-Tannoudji, J. Dupont-Roc, and G. Grynberg, *Atom-Photon Interactions* (John Wiley, New York, 1992), pp. 262–277.
- [15] D. R. Crick *et al.*, *Rev. Sci. Instrum.* **81**, 013111 (2010).
- [16] M. J. Biercuk *et al.*, *Nature (London)* **458**, 996 (2009).
- [17] H. Uys, M. J. Biercuk, and J. J. Bollinger, *Phys. Rev. Lett.* **103**, 040501 (2009).
- [18] M. J. Biercuk *et al.*, *Quantum Inf. Comput.* **9**, 920 (2009).
- [19] R. Ozeri *et al.*, *Phys. Rev. A* **75**, 042329 (2007).